DSPI Filtering Evaluation Method Based on Sobel Operator and Image Entropy

Runkai Zhang, Qiyang Xiao, Ying Du, and Xianyu Zuo

***Abstract*—Evaluating the filtering process of the digital speckle pattern interferometry (DSPI) of a single image by the traditional methods can result in under- or over-filtering. To solve this problem, this paper proposes an image-filtering evaluation method based on the Sobel operator and image entropy. First, the Sobel operator is introduced to convolute a filtered image to obtain a gradient image of a DSPI. Then, by analyzing the gradient image, image entropy is calculated according to the characteristics of the gradient map. Finally, the proposed method is verified by experiments. The experimental results show that the proposed method can quantitatively evaluate the filtering process of the DSPI.**

***Index Terms*—Digital speckle pattern interferometry, continuous filtering process, image entropy, sobel operator.**

I. Introduction

THE digital speckle pattern interferometry (DSPI) is a full-field optical measurement technology, which has the advantages of being contactless, providing a real-time measurement, and having high precision and sensitivity [1]. Due to its characteristics, it has been widely applied to the fields of non-destructive testing [2], [3], biomedical testing [4], [5], precision machinery manufacturing [6], vibration measurement [7], and material's mechanical properties evaluation [8]. The final physical quantity is determined by calculating the interferogram of the DSPI. However, due to the interference of speckle noise, the signal-to-noise ratio of the measured phase image is poor, and the phase measurement sensitivity is low, which severely affects the results and accuracy of subsequent phase unwrapping [9]. Thus, it is necessary to denoise the phase image of the DSPI to improve the signal-to-noise ratio and reduce the measurement error.

Common filtering methods of the DSPI are the mean filtering method and median filtering method [10]. The mean filtering method is a type of linear filtering method, which uses a template to calculate and obtain the gray value of a new pixel, and the new gray value represents the mean value of several pixels around the central pixel in the template. The median filtering method is a type of nonlinear filtering method, which uses the median of the gray value of every pixel in the vicinity of the target pixel to replace the gray value of the target pixel. Compared to the linear filtering methods, the median filtering method can preserve the edge information while denoising, and the calculation process is simple. Both the mean filtering method and the median filtering method can process the DSPI and obtain the denoised image, but these methods are not adaptive and can easily cause over- or under-filtering [11]. Although the speckle index, the peak signal-to-noise ratio, the structural similarity index, and other indicators can be used for the quantitative analysis of a filtering process, these indicators require reference values and are not suitable for quantitative evaluation of a continuous filtering process of a single image [12].

In the related literature, the Sobel operator has been often used to detect image edges and it has the characteristics of fast calculation speed and good detection effect [13]. Thus, it can be used in a variety of situations of image edge detection [14]–[16]. Combining with neural networks, Sobel operator can be applied in bio-medical image [17], face recognition [18], computer aided diagnosis [19], etc. Entropy is a statistical form of features, which can be used to represent the average amount of information in an image [20]. Therefore, it can be applied in many aspects of image processing, such as image segmentation based on local entropy [21], image evaluation [22], [23]. Meanwhile, entropy analysis can also be used in image encryption [24], [25].

Therefore, this paper proposes a filtering evaluation method by combining image entropy and the Sobel operator to analyze the image of the DSPI in continuous filtering process. During the continuous filtering process, sine-and-cosine filtering is used to denoise the image. This type of filtering method firstly transforms the image into cosine and sine maps, and then applies mean filtering to both maps. The reason for this is that the original package phase diagram contains not only noise, but also 2π phase jump. Direct low-pass filtering can remove high-frequency noise, but it will also smooth the phase jump information, resulting in errors in the subsequent unwrapping operation [11]. In the proposed method, a filtered image is convoluted with the Sobel operator to obtain the gradient image of the DSPI, and the image entropy is used to characterize the filtering result. Compared to other filtering evaluation methods, the filtering evaluation method based on the Sobel operator and image entropy is more intuitive. The proposed method can

Manuscript received July 24, 2021; revised September 13, 2021; accepted October 6, 2021. Date of publication October 8, 2021; date of current version October 26, 2021. This work was supported in part by the Young Elite Scientist Sponsorship Program by Henan Association for Science and Technology under Grant 2021HYTP014, and in part by the National Key Research and Development Program under Grant 2016YFF0101802. *(Corresponding author: Qiyang Xiao.)*

Runkai Zhang is with the Miami College of Henan University, Henan University, Kaifeng 475004, China (e-mail: 1838020027@vip.henu.edu.cn).

Qiyang Xiao is with the School of Artificial Intelligence, Henan University, Kaifeng 475004, China (e-mail: yisuoyanyu058@126.com).

Ying Du and Xianyu Zuo are with the School of Computer and Information Engineering, Henan Key Laboratory of Big Data Analysis and Processing, Kaifeng 475004, China (e-mail: hd_duying@163.com; xianyu_zuo@henu.edu.cn).

Digital Object Identifier 10.1109/JPHOT.2021.3118924

quantitatively analyze a continuous filtering process of a single image and improve the degree of automation of the DSPI filtering process. The remainder of the paper is organized as follows: Section II introduces the preliminaries of image entropy and the Sobel operator, Section III describes our evaluation method in detail and illustrate the result of simulation experiment, Section IV presents the experiments on collected DSPI image. We conclude and state the limitation in Section V.

II. Sobel Operator and Image Entropy

A. Sobel Operator

The Sobel operator is a type of discrete difference operator, and it has been mainly used in image edge detection. This operator calculates the gray value of every pixel in the four directions, i.e., in the upper, lower, left, and right directions, and obtains an extreme value at the image edge, thus achieving a significant detection effect. Meanwhile, since a gradient image can be obtained by convoluting an image with the Sobel operator, an edge detection method based on the Sobel operator has the advantages of a simple calculation process, a small amount of calculation, and a fast-processing speed. Therefore, the Sobel operator has been often used in real-time image gradient detection. The symbol ∇f is often used to represent the gradient of an image f at a certain point (x, y). Because the image gradient refers to the changing rates of pixels in the x and y directions, the gradient of an image f can be expressed by a two-dimensional vector as follows:

$$\nabla f\ (x,y) = \begin{bmatrix} g_x \\ g_y \end{bmatrix} = \begin{bmatrix} f(x+1,y) - f(x-1,y) \\ f(x,y+1) - f(x,y-1) \end{bmatrix} \quad (1)$$

where the amplitude and phase angle of ∇f can be respectively expressed as:

$$|\nabla f(x,y)| = \sqrt{{g_x}^2 + {g_y}^2} \quad (2)$$

$$\alpha = \tan^{-1}\left(\frac{g_y}{g_x}\right) \quad (3)$$

Since the Sobel operator uses horizontal and vertical convolution templates to convolute an image, the gradient values of an image f in the horizontal and vertical directions are respectively expressed as:

$$g_x = \begin{bmatrix} -1 & 0 & +1 \\ -2 & 0 & +2 \\ -1 & 0 & +1 \end{bmatrix} * f(x,y) \quad (4)$$

$$g_y = \begin{bmatrix} +1 & +2 & +1 \\ 0 & 0 & 0 \\ -1 & -2 & -1 \end{bmatrix} * f(x,y) \quad (5)$$

Finally, the resulting gradient can be obtained by summarizing the values of g_x and g_y.

B. Image Entropy

The concept of entropy was first introduced in the information theory by C.E. Shannon [26]. Entropy represents a measure of uncertainty of random variables in the information theory, and it is defined as:

$$H\ (X) = -\sum_{x \in X} p(x) \log p(x) \quad (6)$$

where X represents random variables, and it holds that $0 \log 0 = 0$. According to Eq. (6), the greater the uncertainty of random variables is, the greater the information entropy will be, that is, the greater the amount of information contained in an image will be.

Using the information entropy concept, the average information content of an image can be measured by the image entropy. The commonly used image entropy types are histogram entropy [27] and Frieden entropy [28]. In this study, the one-dimensional image entropy that reflects the average information of the whole image is adopted. The main advantage of the one-dimensional image entropy is that it can be used to quantify the amount of information obtained by the human eyes by observing an image. When the outline of an image is clear, and the image content is obvious, the amount of information obtained by the human eyes will increase in comparison to blurred image. In the DSPI analysis, image noise can blur the outline of the image and reduce the amount of information obtained by the human eyes. Therefore, the human eyes can get more information from an image after image filtering, and the image entropy will increase since the image is much clearer after filtering. The entropy $H(f)$ of an image f can be obtained as:

$$H\ (f) = -\sum_{i=0}^{255} p_i \log p_i, \quad (7)$$

where p_i represents the probability of a pixel with a gray value i appearing in an image f.

III. Proposed Methods

A. Evaluation Method

A gradient image can be obtained by convoluting an image and the Sobel operator, and then the image entropy of the gradient image can be calculated. By observing whether the image entropy changing curve enters the platform period to control the number of times of continuous filtering, the phase image can be effectively filtered and denoised. This filtering evaluation method has two main advantages. First, since the Sobel operator is a type of discrete difference operator, the convolution process is simple. Also, the image entropy calculation algorithm needs to traverse an image only once, so the calculation process is fast. Second, the entropy value is higher if a gradient image with less noise is convoluted with the Sobel operator, and the edge of the gradient image is clearer, so the evaluation method is intuitive. The specific steps of the proposed filtering evaluation method are as follows:

1) Firstly, we assume that $f^{(n)}$ represents the DSPI image after the n th filtering iteration. Since the phase of the DSPI image is wrapped between $-\pi$ and π, we can express it as $-\pi < f^{(n)} < \pi$. Then the grayscale values of the DSPI image is expressed as $f^{(n)}(x, y)$ and the image can be transformed to the cosine and sine maps using the

following mapping transformation rules, respectively:

$$F_{sin}^{(n)}\ (x,y) = \left\{ sin\left[f^{(n)}\,(x,y) \times \frac{2\pi}{255} \right] + 1 \right\} \times 127.5 \tag{8}$$

$$F_{sin}^{(n)}\ (x,y) = \left\{ sin\left[f^{(n)}\,(x,y) \times \frac{2\pi}{255} \right] + 1 \right\} \times 127.5 \tag{9}$$

where $F_{sin}^{(n)}(x,y)$ is the gray values of the sine map, and $F_{cos}^{(n)}(x,y)$ is the gray values of the cosine map. In this step, $f^{(n)}(x,y)$ represents the grayscale values of the original image, so it is in the range [0:255]. Also, $F_{sin}^{(n)}(x,y)$ and $F_{cos}^{(n)}(x,y)$ are the grayscale values of the sine maps and cosine maps, so they are in the range [0:255].

2) Apply the mean filtering to the cosine and sine maps, and the results are respectively as follows:

$$F_{sin}^{(n+1)}\,(x,y) = \frac{1}{M \times M} \sum_{k=x-M/2}^{x+M/2} \sum_{l=y-M/2}^{y+M/2} F_{sin}^{(n)}\,(x,y) \tag{10}$$

$$F_{cos}^{(n+1)}\ (x,y) = \frac{1}{M \times M} \sum_{k=x-M/2}^{x+M/2} \sum_{l=y-M/2}^{y+M/2} F_{cos}^{(n)}\,(x,y)\,, \tag{11}$$

where M represents the filtering window size, $F_{sin}^{(n)}(x,y)$ and $F_{cos}^{(n)}(x,y)$ represent the grayscale values of sine and cosine maps after n times of filtering, respectively; $F_{cos}^{(n+1)}$and $F_{sin}^{(n+1)}$ denote the grayscale values of cosine and sine maps after filtering ($n+1$) times of filtering. $F_{sin}^{(n+1)}(x,y)$ and $F_{sin}^{(n+1)}(x,y)$ are the grayscale values of cosine and sine maps after filtering ($n+1$) times of filtering, so they are in the range [0:255].

3) Apply inverse transformation to the filtered sine and cosine maps and obtain the gray values of filtered DSPI as follows:

$$f^{(n+1)}\ (x,y) = \tan^{-1}\left(\frac{F_{sin}^{(n+1)}\,(x,y)}{F_{cos}^{(n+1)}\,(x,y)} \right) \tag{12}$$

In this step, $f^{(n+1)}(x,y)$ denotes the grayscale values of DSPI image after ($n+1$) times of filtering, so they are in the range [0:255].

4) At this step, the Sobel operator is used to convolute the image and obtain the grayscale value matrix of the gradient image as follows:

$$S\left(f^{(n+1)}\,(x,y)\right) = \sqrt{\left(f^{(n+1)}\,(x,y) * g_x\right)^2 + \left(f^{(n+1)}\,(x,y) * g_y\right)^2}, \tag{13}$$

where g_x and g_y represent the templates of the Sobel operator in the horizontal and vertical directions, respectively. In this step, $S(f^{(n+1)}(x,y))$ is grayscale value matrix of the gradient image, so the range of the grayscale values are in [0:255]. In the same way, since $S(f^{(n+1)}(x,y))_x$ and $S(f^{(n+1)}(x,y))_y$ are the gradient in the x and y directions, the grayscale values of them are in the range [0:255].

For the convenience of calculation, the module of the gradient graph is approximated to the sum of the horizontal and vertical component modules. Thus, the modules of the gradient in the x and y directions are respectively expressed as:

$$S\Big(f^{(n+1)}\,(x,y)\Big)_x = \left| g_x * f^{(n+1)}\,(x,y) \right| = \left| \begin{bmatrix} -1 & 0 & +1 \\ -2 & 0 & +2 \\ -1 & 0 & +1 \end{bmatrix} * f^{(n+1)}\,(x,y) \right| \tag{14}$$

$$S\Big(f^{(n+1)}\,(x,y)\Big)_y = \left| g_y * f^{(n+1)}\,(x,y) \right| = \left| \begin{bmatrix} +1 & +2 & +1 \\ 0 & 0 & 0 \\ -1 & -2 & -1 \end{bmatrix} * f^{(n+1)}\,(x,y) \right| \tag{15}$$

Summarizing the modules in the x and y directions, the grayscale value matrix of a filtered image can be obtained as:

$$\begin{aligned} S\left(f^{(n+1)}\,(x,y)\right) &= \left| g_y * f^{(n+1)}\,(x,y) \right| + \left| g_x * f^{(n+1)}\,(x,y) \right| \\ &= \left| \begin{bmatrix} -1 & 0 & +1 \\ -2 & 0 & +2 \\ -1 & 0 & +1 \end{bmatrix} * f^{(n+1)}\,(x,y) \right| \\ &\quad + \left| \begin{bmatrix} +1 & +2 & +1 \\ 0 & 0 & 0 \\ -1 & -2 & -1 \end{bmatrix} * f^{(n+1)}\,(x,y) \right| \end{aligned} \tag{16}$$

5) Calculate the image entropy of a gradient image. According to Eq. (7), the image entropy of the gradient image is calculated by:

$$H\ \left(S\left(f^{(n+1)}\,(x,y)\right)\right) = -\sum_{i=0}^{255} p_i \log p_i \tag{17}$$

where p_i represents the probability of occurrence of a pixel with gray value i in $S(f^{(n+1)}(x,y))$. In this step, since $f^{(n+1)}(x,y)$ and $S(f^{(n+1)}(x,y))$ are grayscale values of images, they are in the range [0:255]. Thus, formula (17) is applied in the range [0:255].

6) Aiming at protecting the image information and reducing the filtering times, whether the entropy changing curve of the image reaches the plateau period can be judged based on the following expressions:

$$H\left(S\left(f^{(n-1)}\,(x,y)\right)\right) > H\left(S\left(f^{(n)}\,(x,y)\right)\right) \tag{18}$$

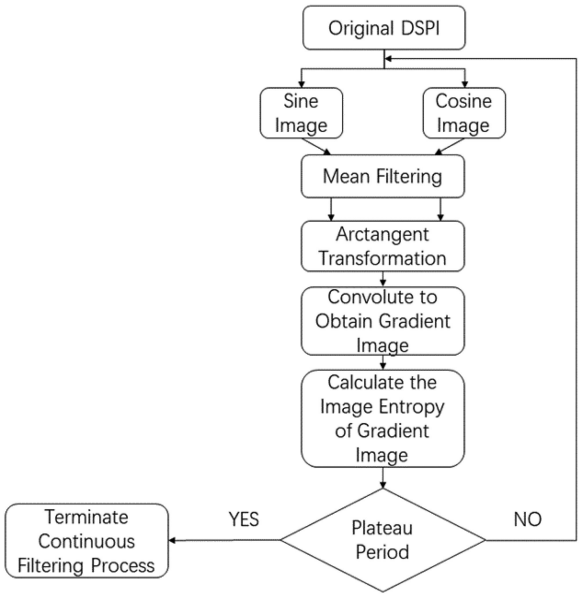

Fig. 1. DSPI filtering evaluation method based on Sobel operator and image entropy.

$$H\left(S\left(f^{(n)}(x,y)\right)\right) < H\left(S\left(f^{(n+1)}(x,y)\right)\right) \quad (19)$$

That is, when the image entropy of the gradient of the DSPI after the $(n+1)$ th filtering is greater than that of the image after the nth filtering, and the image entropy of the gradient of the DSPI after the nth filtering is less than that after the $(n-1)$th filtering, the image entropy changing curve reaches the plateau period, and the continuous filtering process is completed. The significance of reaching a plateau is that it is an important indicator of whether most of the noise is filtered out and the fringe does not have too much offset. The image entropy in plateau period does not change much means that most of the noise has been filtered out compared to original images. Meanwhile, from the definition of image entropy, images in the plateau period contains the same amount of information because the fringe between them has almost no offset, and most of the noise in these images has been filtered out. Thus, it is the appropriate time to stop the filtering.

According to the above steps, our proposed method can be used for the continuous sine-and-cosine filtering process of DSPI image. The flowchart of the proposed method is shown in Fig. 1. As it can be seen from the flowchart, for an original DSPI image, it is divided into a sine image and a cosine image by using mapping transformation. Then, mean filtering is applied to sine image and cosine image, respectively. Thus, after operating arctangent transformation to the sine image and cosine image, a single filtering operation is finished. After that, the filtered image is convoluted with the Sobel operator to obtain gradient image and calculate the image entropy of the gradient image. Finally, drawing the entropy changing curve to observe if the trend of entropy change reaches plateau period. If so, terminate the continuous filtering process and obtain the final image. If not, keep filtering the image until the termination condition is satisfied.

B. Simulation Results

Before applying our method to the continuous filtering process of real and collected DSPI image, we conducted a simulation experiment to verify the effectiveness of the proposed method. The wrapped phase of the DSPI was obtained from the real phase by taking module operation with 2π. The corresponding mathematical expression is as follows:

$$\varphi_2 = mod\left(\varphi_1, 2\pi\right) \quad (20)$$

where φ_2 denotes the wrapped phase, and φ_1 is the real phase.

It was assumed that the wrapped phase was constant in the height direction, i.e., the vertical direction, and the image changed linearly in the horizontal direction. The wrapped image is shown in Fig. 2(a). The Gaussian noise with the mean value of zero and variance of 0.15 was added to the original image to obtain the simulation DSPI with the noise, as shown in Fig. 2(b)

Next, the proposed evaluation method was used to filter the simulation DSPI with the noise. First, the simulation DSPI with the noise was converted to the sine and cosine images. Then, the mean filtering was applied to these images, and filtered images were obtained by using the arctangent transformation. After each filtering, the image was convoluted with the Sobel operator to obtain the gradient map, and the image entropy of the gradient map was calculated. Thus, the filtering process of the simulation image can be reflected by the image entropy changing curve, as shown in Fig. 2(c). In Fig. 2(c), the image entropy changing curve of the simulation DSPI reached its plateau period after 11 times of continuous filtering, and after that, the filtering process terminated. The image after 11 times of continuous filtering is shown in Fig. 2(d). From Fig 2(d), after using the sine-and-cosine filtering method for 11 times, most of the noise in the original image was removed, and the filtering result was almost ideal. The appearance of dark points in the second and fourth fringes is a defect of ordinary sine-and-cosine filtering. This is because in the continuous filtering process, the pixels that form these two dark points are always included in the filtering windows containing relatively many points with lower gray value. To illustrate the filtering result more clearly, the gradient images before and after filtering are compared and displayed in Fig. 2(e) and (f).

As shown in Fig. 2(e), the gradient map of the original image contained more spots in comparison to the filtered image, and the binarization extent of the image was poor. In contrast, the filtered image had a clear edge and contained almost no noise spots, resulting in a preferable binarization performance. According to the concept of image entropy, if the human eyes observe a cleaner image, more information will be obtained. The lines in Fig. 2(f) are clearer than those in Fig. 2(e), which means that the human eyes could obtain more information and indicates that the filtering result was almost ideal.

IV. Experimental Results

A. Experimental Data

The acquired DSPI always contains a large amount of noise, which seriously interferes with the unwrapping and can even

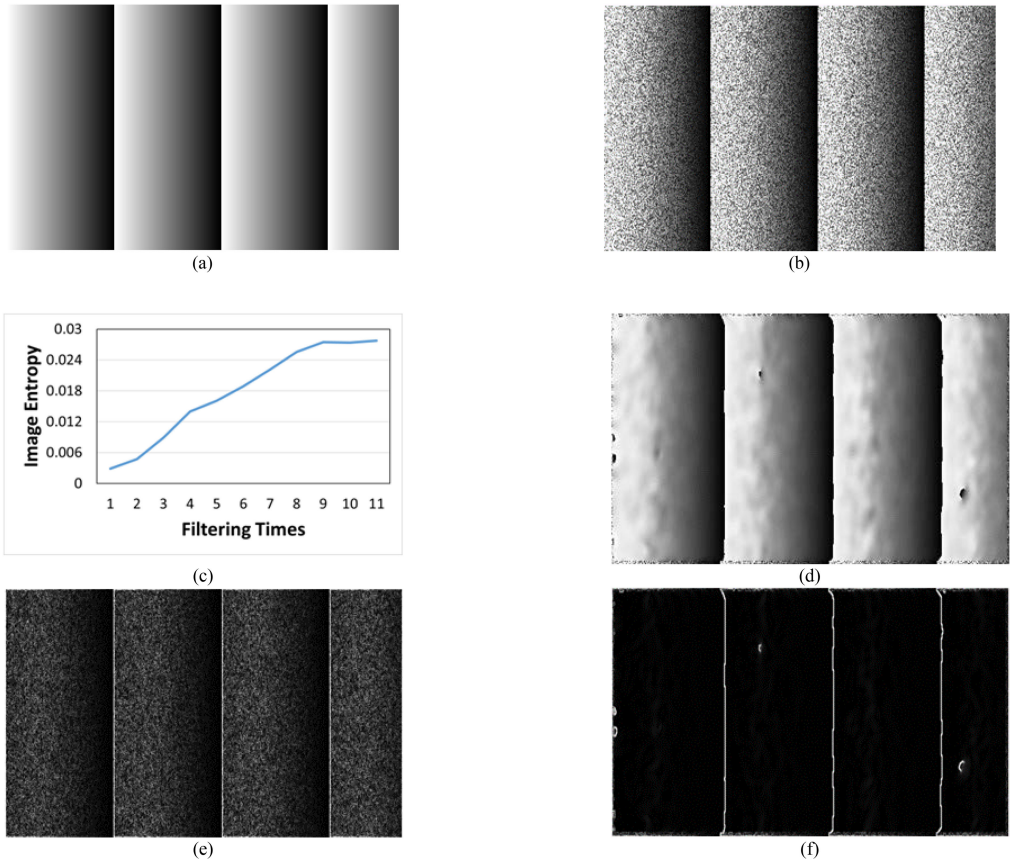

Fig. 2. Evaluation of the continuous filtering of the simulation image. (a) Simulation DSPI without noise; (b) Simulation DSPI with the Gaussian noise; (c) Image entropy changing curve; (d) Image after 11 times of continuous filtering; (e) The gradient image of the original DSPI; and (f) Gradient image after the continuous filtering.

reduce the measurement error. Thus, it is necessary to filter the DSPI to improve measurement accuracy. To verify the proposed method, the in-plane and out-of-plane DSPIs of a deformed object were used, as shown in Fig. 3. In Fig. 3(a) and (b), the in-plane DSPIs of a deformed object at different heights are presented, and in Fig. 3(c) and (d), the out-of-plane DSPIs of the deformed object at different heights are displayed.

The pictures are taken from a disk-shaped piece of copper which was fixed around and centrally loaded. By loading the center of the disk, out-of-plane shape change occurred. Thus, we collected the out-of-plane and in-plane phase maps from different heights. As can be seen from the figure that collected phase maps contained many speckle noises, so it is necessary to suppress the noises for subsequent unwrapping operations.

B. Noisy Images Processing

The sine and cosine filtering method ware used to filter the DSPIs of images presented in Fig. 3. We implemented the proposed evaluation method and continuous filtering process by using MATLAB. The filtering window size was set to 7×7 because too large filtering window size will blur the image and too small filtering window size will make the filtering result not obvious. The sine-and-cosine filtering method has been widely used in the filtering of DSPI due to its capability to retain the information of the original image to the maximum extent and good suppression effect of discrete noise.

After every filtering iteration, the proposed method was used to evaluate the filtering effect. First, the gradient image of a filtered image was obtained by convoluting with the Sobel operator, and then the image entropy of the gradient image was calculated and recorded. Next, the filtering process was repeated, and the image entropy of the gradient image obtained by statistics was drawn into a line graph. The changing curves that show the changing trends of the image entropy under different conditions are shown in Fig. 4.

In Fig. 4, the horizontal axis of the line graphs represents the filtering times, and the vertical axis shows the image entropy of a gradient image. As shown in Fig. 4, although the image entropy values corresponding to different DSPIs are different, the data trends tend to be stable after a certain period, which is consistent with the theoretical analysis presented in Section III. Based on the obtained results, the appropriate filtering times of the DSPIs were 12, 23, 15, and 15, respectively. The gradient images of filtered DSPIs are shown in Fig. 5, where it can be observed that with the increase in the filtering times, the edge of the filtered image was reflected as a set of thin line segments without obvious spots on the gradient map.

The filtered DSPIs are shown in Fig. 6, where the noise spots in each image were greatly reduced compared to the original

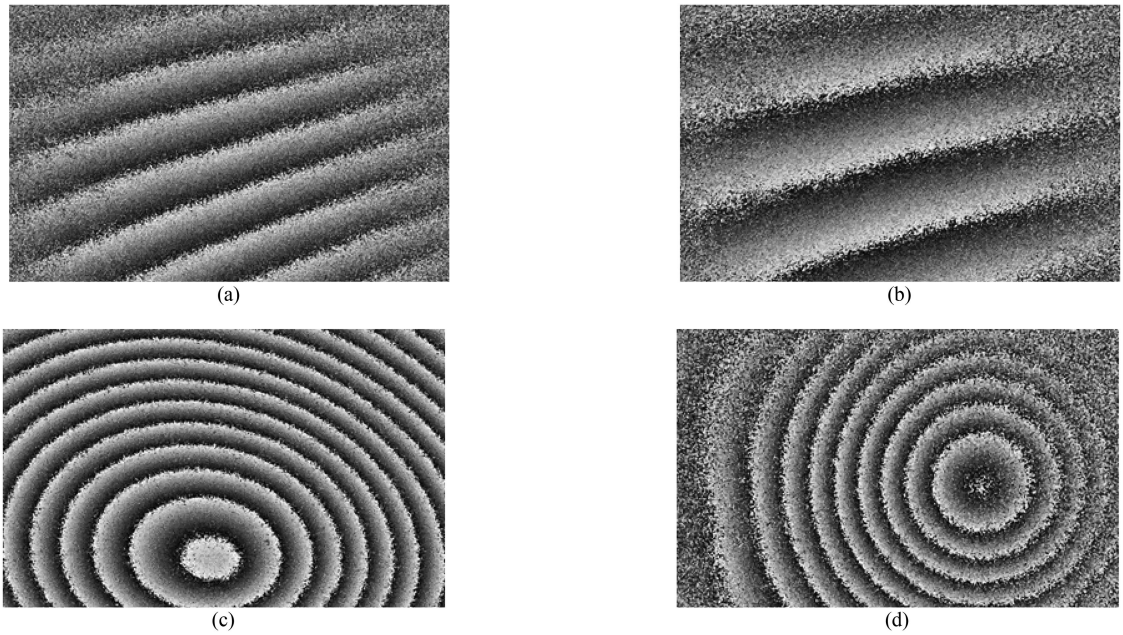

Fig. 3. Experimental DSPI images. (a) In-plane image at a high view height; (b) In-plane image at a low view height; (c) Out-of-plane image at a low view height; and (d) Out-of-plane image at a high view height.

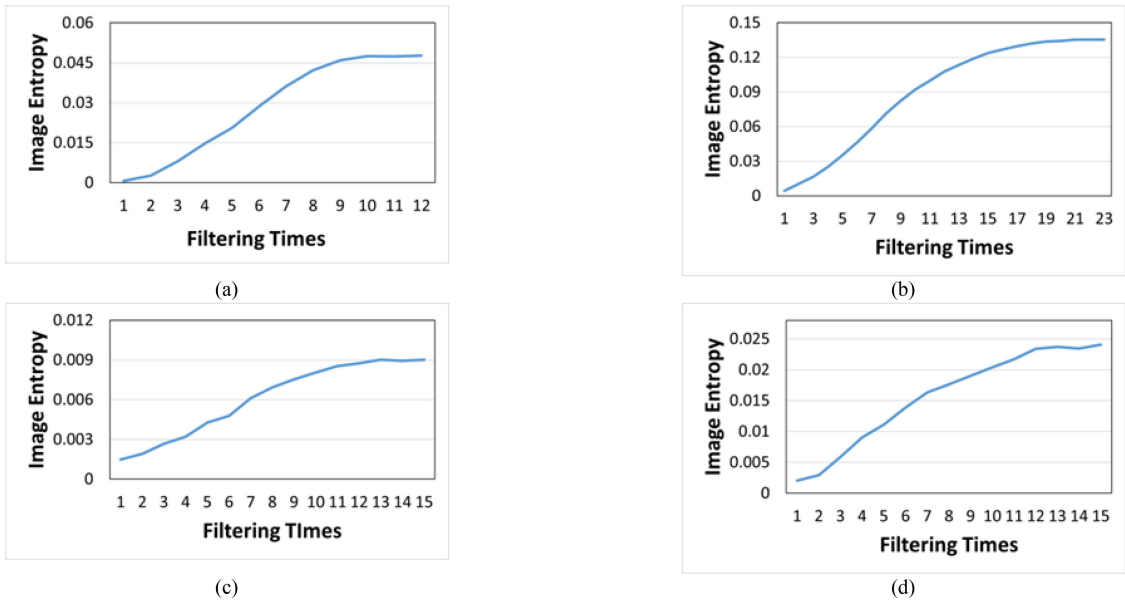

Fig. 4. Image entropy changing curves. (a) Image entropy changing curve at a high view height of the in-plane image; (b) Image entropy changing curve at a low view height of the in-plane image; (c) Image entropy changing curve at a low view height of the out- of-plane image; and (d) Image entropy changing curve at a high view height of the out-of-plane image.

image, and distortion was low; thus, the filtering effect was good. Although the edge in Fig. 6(d) contains certain noise spots, the effect of subsequent filtering would be poor, and the image would be distorted, which could result in the loss of the original information.

By observing the experimental results, we can briefly conclude that the proposed method can not only quantitatively evaluate the filtering effect but also adaptively judge whether image filtering is completed.

C. *Unwrapping Evaluation*

To further verify the effectiveness of the proposed method and the accuracy of the DSPI filtering, the unwrapping algorithm was used to process the filtered images. The unwrapping algorithm we used is the least-square unwrapping method [29]. The criterion of the least-square unwrapping method is to minimize the difference between the discrete partial differential of the wrapping phase and the discrete partial differential of the unwrapping

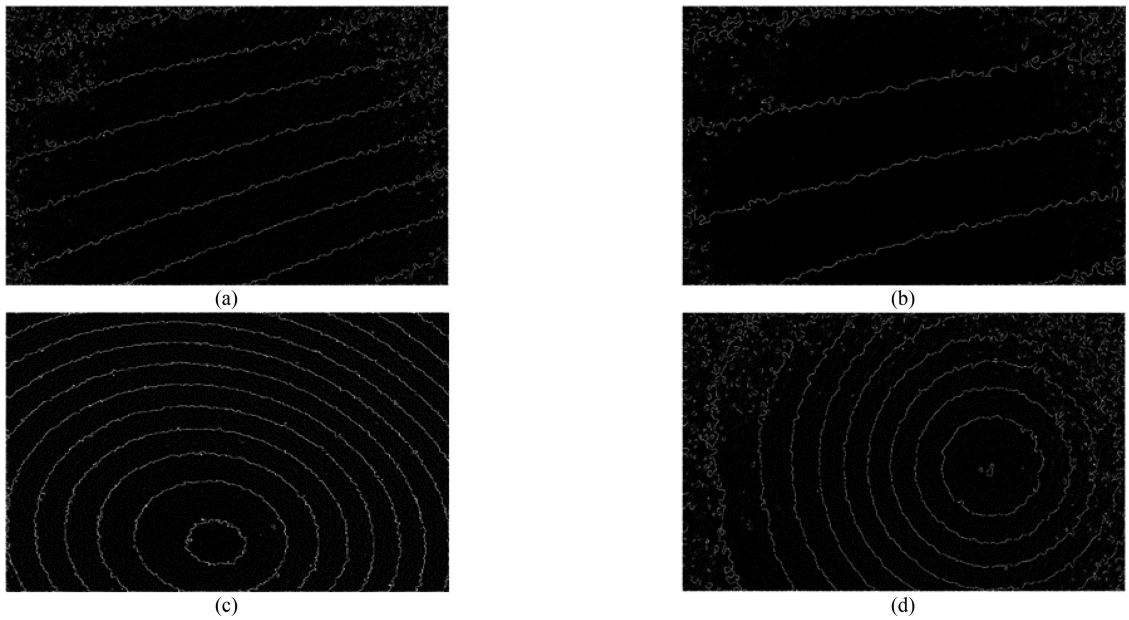

Fig. 5. Gradient images after the continuous filtering process. (a) Gradient image of the filtered in-plane image at a high view height; (b) Gradient image of the filtered in-plane image at a low view height; (c) Gradient image of the filtered out-of-plane image at a low view height; and (d) Gradient image of the filtered out-of-plane image at a high view height.

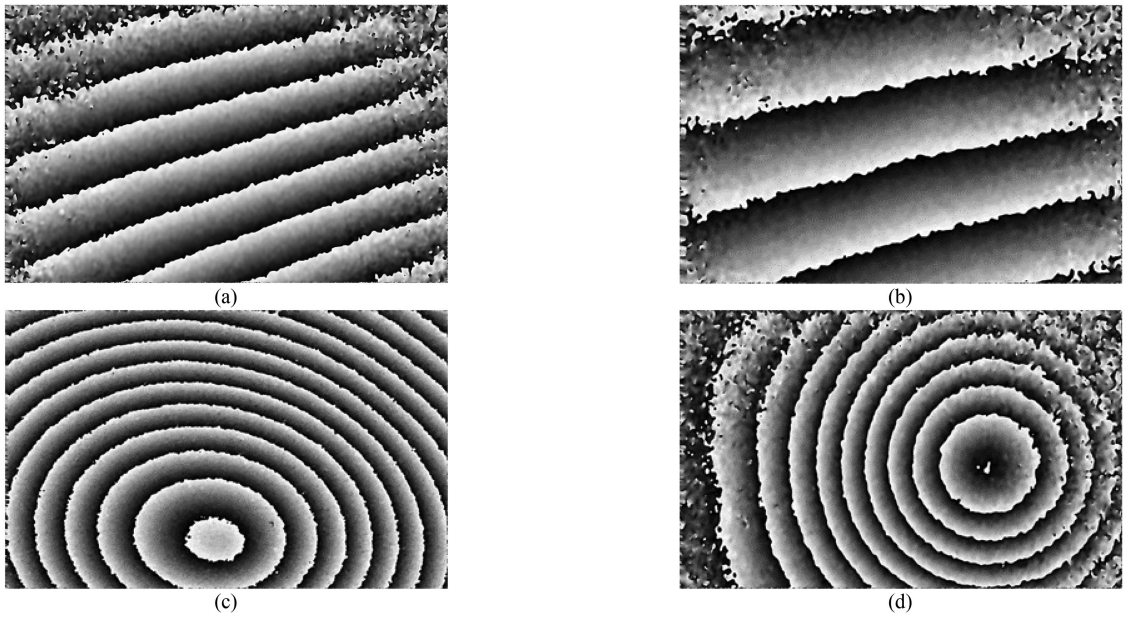

Fig. 6. DSPI images after the continuous filtering process. (a) DSPI at a high view height of the in-plane image after the continuous filtering process; (b) DSPI of a low view height of the in-plane image after the continuous filtering process; (c) DSPI at a low view height of the out-of-plane image after the continuous filtering process; and (d) DSPI at a high view height of the out-of-plane image after the continuous filtering process.

phase. Least-square unwrapping method is a simple algorithm since it has fast operation speed and requires small amount of memory. Due to the property of noise sensitivity, it is suitable for our evaluation experiment. The obtained unwrapping images are shown in Fig. 7., where each unwrapping image was continuous and clear without obvious noise spots. The fringe change in the unwrapped image's phase was relatively smooth after unwrapping, and there was neither unwrapping failure nor error area.

The unwrapping processing of the filtered images further illustrated that the proposed method could achieve a good filtering effect for common DSPIs in engineering practice, and the phase jump information of the original image was not lost when most of the noise was filtered out.

Consequently, the proposed method can judge the filtering effect for common DSPIs in the engineering field. Meanwhile, it can judge the completion of the continuous filtering processing of a single image, which fully proves the effectiveness of the

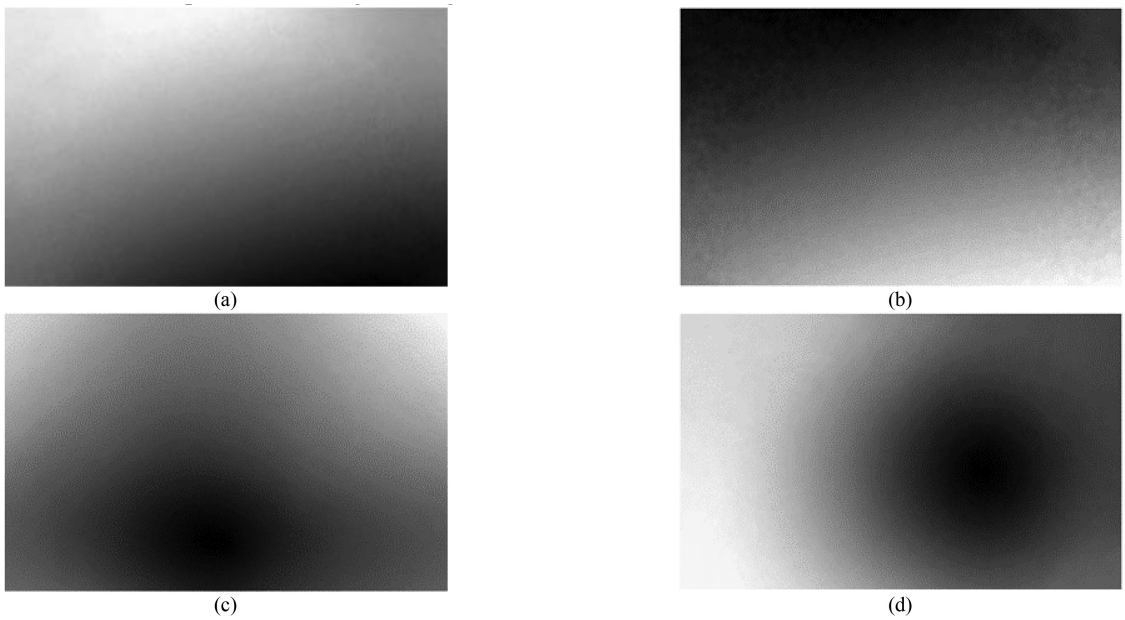

Fig. 7. Unwrapping images under different conditions. (a) Unwrapping image of the in-plane image at a high view height; (b) Unwrapping image of the in-plane image at a low view height; (c) Unwrapping image of the out-of-plane image at a low view height; and (d) Unwrapping image of the out-of-plane image at a high view height.

TABLE I
CONTINUOUS FILTERING TIMES OF DIFFERENT EVALUATION METHODS

DSPIImage	Smooth Spline Filtering	Entropy Method
In-plane image at a high view height	4	12
In-plane image at a low view height	6	23
Out-of-plane image at a low view height	5	15
Out-of-plane image at a high view height	5	15

proposed filtering evaluation method based on the Sobel operator and image entropy.

D. Comparison Experiment

To illustrate the advance of the proposed method, we compared it with the work proposed by Zhao *ET AL.* in 2018, which is an almost state-of-the-art evaluation method [30]. The work done by these researchers proposed an evaluation method based on smooth spline fitting. First, we used their method in the continuous filtering process to decide the times of filtering. The times of filtering are shown in Table I.

From the above table, we considered that evaluation method based on smooth spline fitting may cause under-fitting. Thus, we followed their approach and the phase distribution on the main diagonal is selected as the fitting object. The fitting results is illustrated in Fig. 8.

From above results, it is easy to find out that there are still many noisy spots along the main diagonal, which is a symbol of under-filtering. In comparison to Fig. 8(d), Fig. 8(c) contains obviously more noise between zero to 300 of the x-axes. In Fig. 8(g), the existence of noise around 1000 of the x-axes even affect the result of smooth spline fitting compared with Fig. 8(h).

E. Discussion

Overall, for different images in Fig. 6, most of the noises contained can be reduced after certain times of filtering. From Fig. 5, we can conclude that the edges in gradient maps are clear and distinct after using the proposed evaluation method in continuous filtering process. Meanwhile, there is a small amount of noise existing in the edge of the image, which is the defect of mean filtering itself. On the other hand, as can be seen from the results of unwrapping evaluation, although some noises are still contained in the image, the unwrapping results show that they have almost no negative effect to the unwarping results.

Compared with another evaluation method of continuous filtering process, our proposed method can autonomously select appropriate filtering times, and make the result of smooth spline fitting more accurately.

However, to see what happens to the images and entropy plots after the plateau period, we take Fig. 3(c) as an example and illustrate the subsequent situation.

Firstly, we plotted the entropy changing curve during 60 times of filtering, as shown in Fig. 9.

In overall, it can be seen from the above figure that the entropy plot continues to rise after a plateau period. In the plot, the plateau period starts from about the 15th filtering, and ends at about the 33rd filtering, which confirms our judgement that 15 is the best times of filtering for Fig. 3(c) in the paper because the plateau period starts there. As the curve rises, it seems the amount of information we get from the image will also increase according to the definition of image entropy. However, when we carefully observe the subsequent images, we find that this

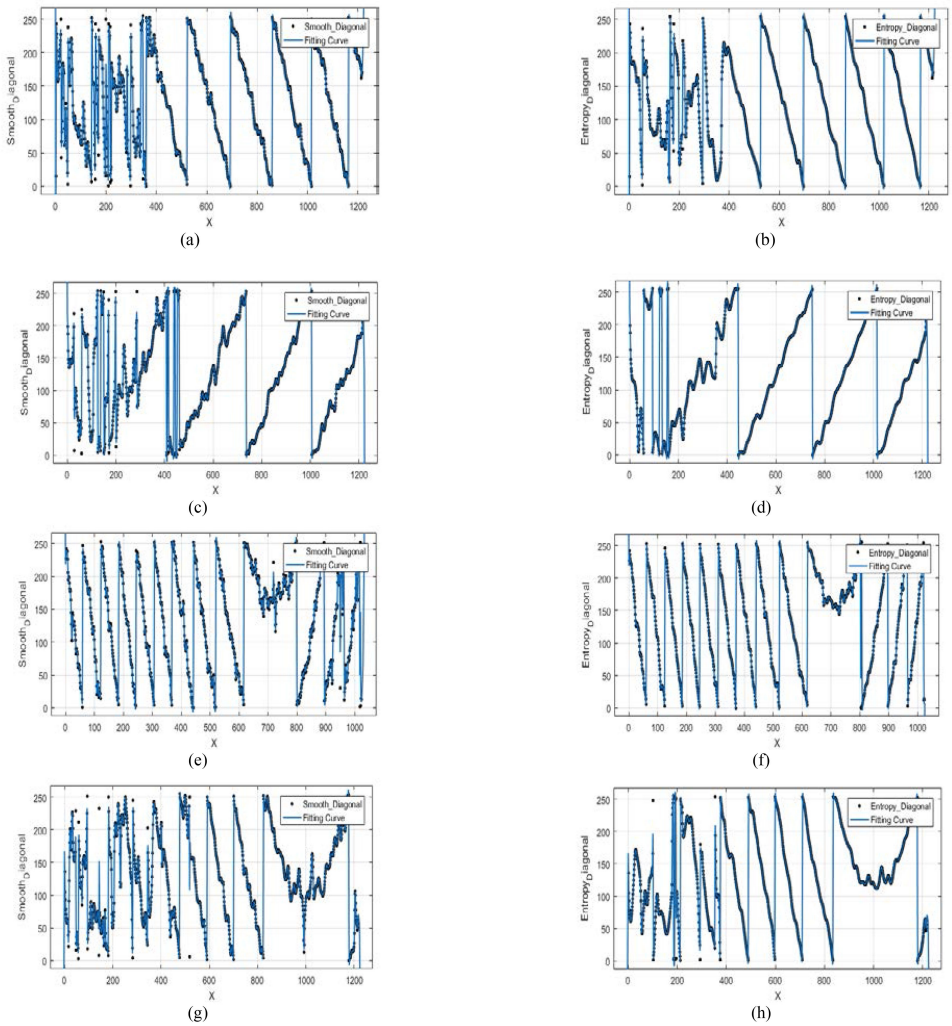

Fig. 8. Phase distribution on the main diagonal. (a) Phase distribution on the main diagonal of in-plane image at a high view height by using method of Zhao *et al.*; (b) Phase distribution on the main diagonal of in-plane image at a high view height by using our method; (c) Phase distribution on the main diagonal of in-plane image at a low view height by using method of Zhao *et al.*; and (d) Phase distribution on the main diagonal of in-plane image at a low view height by using our method; (e) Phase distribution on the main diagonal of out-of-plane image at a low view height by using method of Zhao *et al.*; (f) Phase distribution on the main diagonal of out-of-plane image at a low view height by using our method (g) Phase distribution on the main diagonal of out-of-plane image at a high view height by using method of Zhao *et al.*; and (h) Phase distribution on the main diagonal of out-of-plane image at a high view height by using our method.

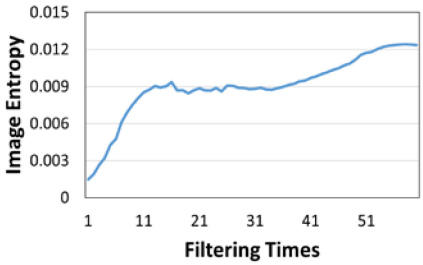

Fig. 9. Entropy changing curve of Fig. 3(c) in the paper during 60 times of filtering.

is not the case. The subsequent images are shown in Fig. 10. It can be seen from the figures that the left edge of the DSPI image gradually become distorted. This distortion also appears in the upper left edge of the DSPI, but more slightly. Although the fringes of the image become very smooth, the increasing distortion is something that we are not willing to see. However, this phenomenon provides some guidance to our next research.

V. Conclusion

To overcome the limitation that the traditional filtering evaluation methods cannot provide continuous filtering of DSPI of a single image, this paper proposes a filtering evaluation method based on the Sobel operator and image entropy. Compared with other evaluating methods, our proposed method creates a filtering process which has excellent visibility due to the usage of Sobel operator. Moreover, by calculating the image entropy of DSPI, a more natural way to filter is built. According to the simulation and experimental results, the following conclusions can be drawn:

The proposed filtering evaluation method based on the Sobel operator and image entropy can not only quantitatively evaluate the filtering effect but also judge whether image filtering is completed automatically.

The proposed filtering evaluation method can be used for automatic filtering of DSPI, achieving a good filtering effect.

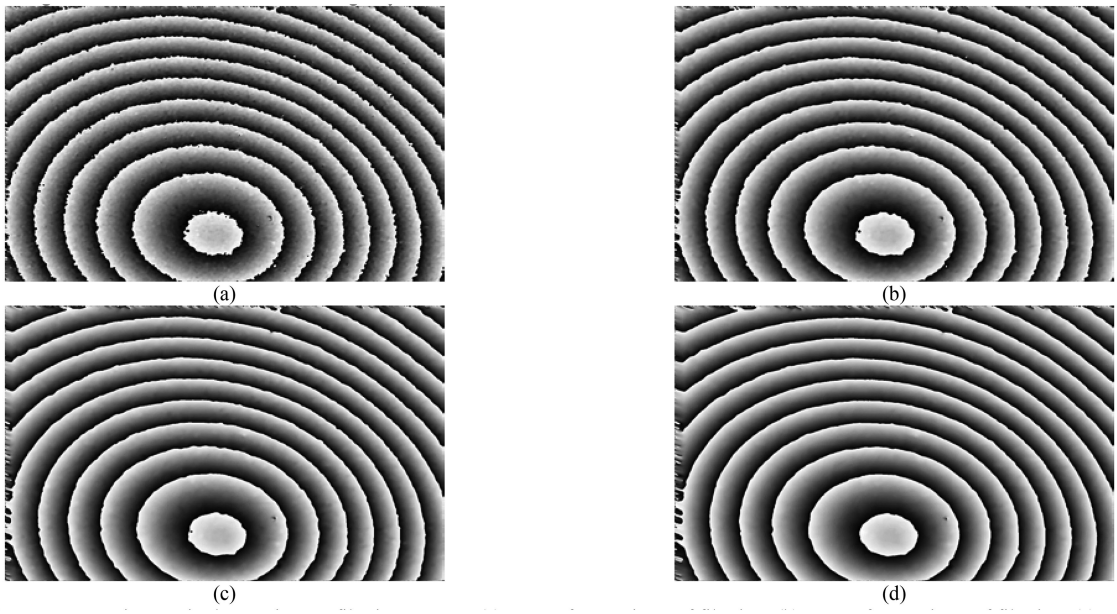

Fig. 10. Subsequent DSPI images in the continuous filtering process. (a) DSPI after 15 times of filtering; (b) DSPI after 30 times of filtering; (c) DSPI after 45 times of filtering; and (d) DSPI after 60 times of filtering.

REFERENCES

[1] Y. Su *et al.*, "Theoretical analysis on performance of digital speckle pattern: Uniqueness, accuracy, precision, and spatial resolution," *Opt. Exp.*, vol. 27, pp. 22439–22474, 2019.

[2] C. L. Song, A. S. Prasad, G. D., V. Matham, and M. K. Chan, "Non-Destructive testing on optofluidic lens using speckle Referencing-DSPI," in *Proc. Int. Conf. Inform.*, Phuket, Thailand, Apr. 24, 2016, pp. 105–109.

[3] H. J. Shu and G. L. Yi, "Study on non-destructive testing of aerial complex material by DSPI," *Mater. Sci. Forum*, vol. 61, pp. 837–840, 2007.

[4] S. P. Rubnikovich, Y. A. Denisova, and N. A. Fomin, "Digital laser speckle technologies in measuring blood flow in biotissues and the stressed-strained state of the maxillodental system," *J. Eng. Phys. Thermophys.*, vol. 90, pp. 1513–1523, 2017.

[5] K. Udayakumar, N. U. Sujatha, and R. A. Ganesan, "Quantitative assessment of soft tissue deformation using digital speckle pattern interferometry: Studies on phantom breast models," *J. Med. Imag.*, vol. 4, 2017, Art. no. 016001.

[6] S. J. Wu, J. Yang, W. X. Li, F. Wi, and M. L. Dong, "Precision roll angle measurement based on digital speckle pattern interferometry," *Meas. Sci. Technol.*, vol. 30, 2019, Art. no. 045005.

[7] K. Creath and Å. S. Gudmunn, "Vibration-observation techniques for digital speckle-pattern interferometry," *J. Opt. Soc. Amer. A - Opt. Image Sci. Vis.*, vol. 2, pp. 1629–1636 1985.

[8] S. Toyooka and X. L. Gong, "Digital speckle pattern interferometry for observing the entire process of plastic deformation of a solid object," *Japanese J. Appl. Phys.*, vol. 34, pp. L1666–L16668, 2014.

[9] J. Chen, L. Yang, and J. D. Luo, "Research on speckle interference image filtering method for small diameter thin wall tube surface quality detection," *Sci. Technol. Vis.*, vol. 15, pp. 50–54, 2020.

[10] X. L. Wang, L. Li, and H. M. Xin, "Comparative study on noise reduction techniques of speckle interference fringes," *Modern Electron. Technol.*, vol. 38, pp. 63–66, 2015.

[11] H. Y. Jiang, M. L. Dai, Z. L. Su, F. J. Yang, and X. Y. He, "An adaptive sine/cosine filtering algorithm based on speckle phase fringe orientation," *Acta Optica Sinica*, vol. 37, pp. 81–88, 2017.

[12] B. Cha, J. L. Jiang, G. M. Liu, S. G. Han, and Z. Huang, "Adaptive weighted mean filtering algorithm for removing high density salt and pepper noise," *J. Chizhou Univ.*, vol. 34, pp. 43–45, 2020.

[13] R. Tian, G. L. Sun, X. C. Liu, and B. W. Zheng, "Sobel edge detection based on weighted nuclear norm minimization image denoising," *Electronics*, vol. 10, pp. 655–655, 2021.

[14] H. D. Ren, L. Wang, and S. M. Zhao, "Efficient edge detection based on ghost imaging," *OSA Continuum*, vol. 2, pp. 64–73, 2019.

[15] R. Chetia, S. M. B. Boruah, and P. P. Sahu, "Quantum image edge detection using improved sobel mask based on NEQR," *Quantum Inf. Process.*, vol. 20, 2021, Art. No 21.

[16] H. D. Ren, S. M. Zhao, and J. Gruska, "Edge detection based on single-pixel imaging," *Opt. Exp.*, vol. 26, pp. 5501–5511, 2018.

[17] M. Vardhana, N. Arunkumar, S. Lasrado, and E. G. R. G. Abdulhay, "Convolutional neural network for bio-medical image segmentation with hardware acceleration," *Cogn. Syst. Res.*, vol. 50, pp. 10–14, 2018.

[18] X. L. Tang, X. G. Wang, J. Hou, H. F. Wu, and D. Liu, "An improved sobel face gray image edge detection algorithm," in *Proc. 39th China Control Conf.*, Shenyang, China, Jul. 27, 2020, pp. 860–864.

[19] H. L. Yan, H. J. Lu, M. C. Ye, K. Yan, Q. Jin, and Y. G. Xu, "Lung nodule segmentation combining sobel operator and mask R-CNN," *J. Chin. Comput. Syst.*, vol. 41, pp. 161–165, 2020.

[20] J. Steven amd and M. Andrea, "Salient slices: Improved neural network training and performance with image entropy," *Neural Computation*, vol. 32, pp. 1222–1237, 2020.

[21] F. Hržić, I. Štajduhar, S. Tschauner, E. Sorantin, and J. Lerga, "Local-entropy based approach for X-ray image segmentation and fracture detection," *Entropy*, vol. 21, 2019, Art. no. 338.

[22] J. Liu, M. Xu, X. Xu, and Y. Huang, "Nonreference image quality evaluation algorithm based on wavelet convolutional neural network and information entropy," *Entropy*, vol. 21, 2019, Art. no. 1070.

[23] X. Li, J. Wang, M. Li, Z. Peng, and X. Liu, "Investigating detectability of infrared radiation based on image evaluation for engine flame," *Entropy*, vol. 21, 2019, Art. no. 946.

[24] S. Moafimadani, Y. Chen, and C. Tang, "A new algorithm for medical color images encryption using chaotic systems," *Entropy*, vol. 21, 2019, Art. no. 577.

[25] A. K. Farhan, N. M. G. Al-Saidi, A. T. Maolood, F. Nazarimehr, and I. Hussain, "Entropy analysis and image encryption application based on a new chaotic system crossing a cylinder," *Entropy*, vol. 21, 2019, Art. no. 958.

[26] C. E. Shannon, "A mathematical theory of communication," *Mobile Comput. Commun. Rev.*, vol. 5, pp. 3–55, 2001.

[27] T. Pun, "A new method for gray-level picture thresholding using the entropy of the histogram," *Signal Process.*, vol. 2, pp. 223–237, 1985.

[28] B. R. Frieden, "Restoring with maximum likelihood and maximum entropy," *J. Opt. Soc. Amer.*, vol. 62, pp. 511–518, 1972.

[29] D. C. Ghiglia and L. A. Romero, "Robust two-dimensional weighted and unweighted phase unwrapping that uses fast transforms and iterative methods," *J. Opt. Soc. Amer.*, vol. 11, pp. 107–117, 1994.

[30] Q. H. Zhao, Y. H. Wang, X. Y. Gao, F. Y. Sun, P. X. Yan, and L. X. Yang, "Filtering evaluation method of phase images based on smooth spline fitting," *Acta Optica Sinica*, vol. 38, pp. 204–210, 2018.